HETEROCYCLES, Vol. 94, No. 1, 2017, pp. 131 - 139. © 2017 The Japan Institute of Heterocyclic Chemistry
Received, 4th November, 2016, Accepted, 21st December, 2016., Published online, 26th December, 2016
DOI: 10.3987/COM-16-13608

MOLECULAR STRUCTURE AND SPECTROSCOPIC PROPERTIES OF [2,3,9,10,16,17,23,24-OCTAKIS(3-CARBOXYPHENOXY)PHTHALOCYANINATO-κ^4N](PYRIDINE-κN)ZINC(II) PYRIDINE OCTASOLVATE

Rei Fujishiro,[1] Hayato Sonoyama,[1] Yuki Ide,[1] Shigeki Mori,[2*] Tamotsu Sugimori,[3] Atsushi Nagai,[4] Katsumi Yoshino,[5] Mikio Nakamura,[6] and Takahisa Ikeue[1*]

[1] Department of Chemistry, Graduate School of Science and Engineering, Shimane University, 1060, Nishikawatsu, Matsue, 690-8504, Japan. [2] Advanced Research Support Center, Ehime University, 2-5 Bunkyo-cho, Matsuyama, 790-8577, Japan. [3] Division of Chemistry, Graduate School of Medicine and Pharmaceutical Science, University of Toyama, 2630, Sugitani, Toyama, 930-0194, Japan. [4] Department of Laboratory Medicine, School of Medicine, Shimane University, Izumo, Japan. [5] Shimane Institute for Industrial Technology, 1, Hokuryo, Matsue, 690-0816, Japan. [6] Department of Chemistry, Faculty of Science, Toho University, Funabashi, 274-8510, Japan. E-mail : ikeue@riko.shimane-u.ac.jp (T. Ikeue), mori.shigeki.mu@ehime-u.ac.jp (S. Mori).

Abstract – The title complex, [2,3,9,10,16,17,23,24-octakis(3-carboxyphenoxy)-phthalocyaninato-*k* ^{4}*N*](pyridine-*kN*)zinc(II)pyridine octasolvate abbreviated as [ZnPc(3-$CO_2H)_8$(Py)]·8(Py) (**2**), has been obtained by recrystallization of [ZnPc(3-$CO_2H)_8$] (**1**) from pyridine. Molecular structure of **2** determined by X-ray crystallography exhibits the anticipated N_5 square pyramidal coordination structure around zinc(II) ion, where the average Zn-N(Pc) and Zn-N(Py) bond lengths are 2.027(4) Å and 2.121(4) Å, respectively. The deviation of the zinc(II) ion from the phthalocyanine N_4 plane is 0.417 Å. Eight pyridine molecules are involved in the hydrogen bonding with the carboxylic acid moieties of phenoxy rings in a 1:1 mode. Two discrete phthalocyanine molecules in a unit cell are stacked in a back-to-back fashion with an interplanar distance of 3.376 Å. Pyridine solutions of **1** exhibit well-resolved ^{1}H NMR, UV-Vis, and fluorescent spectra, suggesting that **1** exists as pyridine ligated monomeric species.

Phthalocyanines and their metal complexes have attracted much attention because of their characteristic physicochemical properties ascribed to their extended π-conjugation system. One of such characteristics is their intensive Q band in 670-750 nm region with a typical molar extinction coefficient(ε) of ca. 10^5 $M^{-1}cm^{-1}$.[1] Phthalocyanines and their metal complexes have been used as important materials in industry such as dye-stuffs, photoconductivity agents in photocopying machines, photosensitizers in photodynamic therapy (PDT), and so forth.[2,3] Phthalocyanines used as thin films or those adsorbed on inorganic semiconductors have potential applications in organic photovoltaics or dye-sensitized solar cells.[4] Phthalocyanines having hydrophilic groups are potentially useful as water-soluble materials. Vicente et al. reported the synthesis of zinc(II) phthalocyanine complex having sixteen carboxyl groups at the eight phenoxy groups attached to the peripheral β-positions, and examined the photophysical properties together with the activity as a sensitizer for the photodynamic therapy.[5,6]

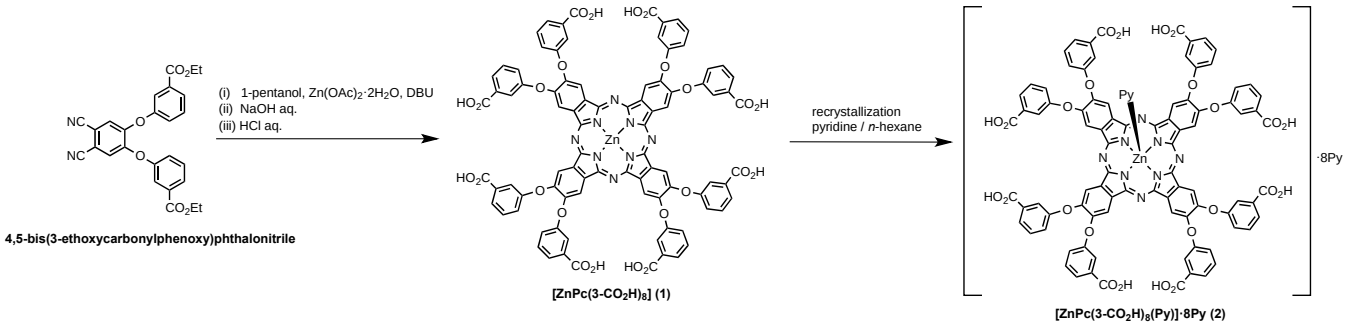

Scheme 1. Synthetic route of zinc(II) phthalocyanines (**1** and **2**)

Although there are ample examples on water-soluble phthalocyanines carrying several carboxylic or sulfonic acid moieties, their crystal structures have rarely been reported probably due to the difficulty for obtaining suitable crystals for the X-ray analysis. In this paper, we will report the crystal and molecular structures of the title complex $[ZnPc(3\text{-}CO_2H)_8(Py)]\cdot 8(Py)$ (**2**) converted from readily obtainable $[ZnPc(3\text{-}CO_2H)_8]$ (**1**) by recrystal- lization from pyridine solution. We will also report the solution properties of **1** as examined by ^1H NMR, UV-Vis, and fluorescence spectroscopy.

Scheme 1 shows the synthetic route to prepare **1** and **2**. Complex **1** was characterized by ^1H NMR, UV-Vis, MALDI-TOF-Mass, and elemental analysis as described in the experimental section of supporting information. Four-coordinate **1** was converted to pyridine ligated five-coordinate **2** by recrystallization from pyridine / *n*-hexane solution. The crystals thus formed were suitable for X-ray structure analysis. The crystal data for **2** together with the data collection details are given in Table S1. Figure 1 shows the ORTEP diagram of **2** together with the atom labeling. The axially coordinated pyridine molecule and eight 3-carboxyphenoxy groups are clearly observed. In addition, eight solvated pyridine molecules have involved in the hydrogen bonds with the carboxylic acid moieties (averaged O-N

= 2.66 Å). Table 1 shows the selected bond distances, bond angles, and dihedral angles. The bond length of the axially coordinated pyridine nitrogen to the zinc atom Zn-N_{ax} is 2.121(4) Å, while the average bond length of phthalocyanine nitrogen to the zinc atom Zn-N_{eq} is 2.027(4) Å. The zinc(II) ion is located in a distorted square-pyramidal coordination geometry and is displaced from the least-squares N_4 plane of phthalocyanine by 0.417 Å toward the axially coordinated pyridine N atom. These values are comparable to the corresponding values in analogous [Zn(Pc)(4-NH_2Py)], where Zn-N_{ax} and the averaged Zn-N_{eq} length are 2.092 and 2.032 Å, respectively, and the out-of-plane displacement of the zinc(II) ion is 0.446 Å.[7] The dihedral angle between phthalocyanine N_4 plane and the plane of the coordinated pyridine ligand is

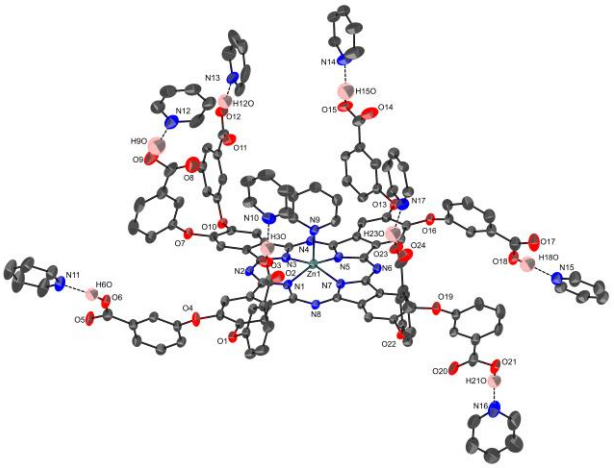

Figure 1. ORTEP view of **2**. Hydrogen atoms except for the carboxylic protons are omitted for clarity. The thermal ellipsoids are shown at the 30% probability level.

Table 1. Selected distances (Å), angles (°), and dihedral angles (°) for **2**

Zn(1)-N_{eq}(1)	2.033(4)	N_{eq}(1)-Zn(1)-N_{eq}(3)	87.4(2)	C(4)-O(1)-C(9)	117.9(4)
Zn(1)-N_{eq}(3)	2.024(4)	N_{eq}(1)-Zn(1)-N_{eq}(5)	156.2(2)	C(5)-O(4)-C(16)	119.3(4)
Zn(1)-N_{eq}(5)	2.018(4)	N_{eq}(1)-Zn(1)-N_{eq}(7)	88.0(1)	C(26)-O(7)-C(31)	116.9(4)
Zn(1)-N_{eq}(7)	2.034(5)	N_{eq}(3)-Zn(1)-N_{eq}(5)	87.8(2)	C(27)-O(10)-C(38)	117.6(4)
Zn(1)-N_{ax}(9)	2.121(4)	N_{eq}(3)-Zn(1)-N_{eq}(7)	156.4(2)	C(48)-O(13)-C(53)	116.8(4)
Zn-N_{eq}(ave.)	2.027(4)	N_{eq}(5)-Zn(1)-N_{eq}(7)	87.1(1)	C(49)-O(16)-C(60)	118.1(4)
$\lvert\Delta Zn\rvert^a$	0.417	N_{eq}(1)-Zn(1)-N_{ax}(9)	101.7(2)	C(70)-O(19)-C(75)	120.2(4)
θ^b	85.92	N_{eq}(3)-Zn(1)-N_{eq}(9)	103.3(2)	C(71)-O(22)-C(82)	118.8(3)
$d_1{}^c$	3.376	N_{eq}(5)-Zn(1)-N_{eq}(9)	102.1(2)	C-O-C (ave.)	118.2(4)
$d_2{}^d$	4.774	N_{eq}(7)-Zn(1)-N_{eq}(9)	100.3(2)		

[a] The distance between the Zn(II) atom and the least-square Pc plane defined by the four N4 atoms(N1, N3, N5, and N7) of the phthalocyanine core.
[b] The dihedral angle between the least-square Pc plane and the plane of the coordinated pyridine molecule.
[c] The interplanar distances of back-to-back fashion Pc dimer.
[d] The slipped distances between the centroids of Pc plane defined by the four N4 atoms(N1, N3, N5, and N7) of the phthalocyanine core.

85.92°, indicating that the pyridine ligand is almost perpendicular to the phthalocyanine plane. The pyridine ligand is aligned much closer to the diagonal N(*meso*)-N(*meso*) axis than to the diagonal N(isoindole)- N(isoindole) axis; the orient- ation angle of the pyridine ligand against N(*meso*)-N(*meso*) axis is 9.3°. The perpendicular displacement of each atom from the least-squares N_4 plane of phthalocyanine is given in Figure S1. The phthalocyanine ring is slightly deformed; the maximum deviation of the pyrrole β-carbon atom is 0.25 Å. The result is in sharp contrast to the zinc(II) phthalocyanine complex bearing eight phenyl substituents at the α-positions, *i.e.*, 1-, 4-, 8-, 11-, 15-, 18-, 22-, and 25-positions. This complex exhibits a strongly saddled deformation due to the severe steric

repulsion between two neighboring phenyl rings. Thus, the maximum deviation of the pyrrole β-carbon atom reaches as much as 1.18 Å.[8] The crystal packing diagram of **2** is shown in Figure 2(a). A unit cell contains two discrete phthalocyanine complexes. These molecules stack in a back-to-back fashion with an interplanar distance of 3.376 Å and zinc-zinc distance of 5.400 Å. The phthalocyanine planes are not completely overlapped but slipped by 3.605 Å, suggesting a strong π–π interaction between two molecules. Figure 2(b) shows various interactions within a dimer and also with neighboring dimers. Close inspection of Figure 2(b) has revealed that the crystal structure of **2** is stabilized by hydrogen bonds and π–π interactions. Solvated pyridine molecules are playing important role in fixing the crystal structure. Thus, in addition to the π–π interaction between two phenoxy groups in the same dimer, two solvated pyridine molecules also exhibit the π–π interactions as shown in the red frame. The interplanar distances in these interactions are ca. 3.5 Å and ca. 3.6 Å, respectively. The blue frame exhibits the π–π interactions between the coordinated pyridine ligand and the solvated pyridine molecule which is hydrogen bonded with carboxyl group of the neighboring dimer. The interplanar distance between these pyridine rings is ca. 3.4 Å. Figure 2(b) also shows that a dimer interacts with the neighboring dimers through π–π interactions between two phenoxy groups as shown in the green frame. The π–π interaction is also observed between two solvated pyridine molecules both of which are hydrogen bonded with carboxyl groups of the different dimers; the interplanar distances are ca. 3.4 Å in both cases. Due to these interactions, the crystals of **2** construct infinite one dimensional layers along the a axis. Crystal packing diagram is also given in Figure S2.

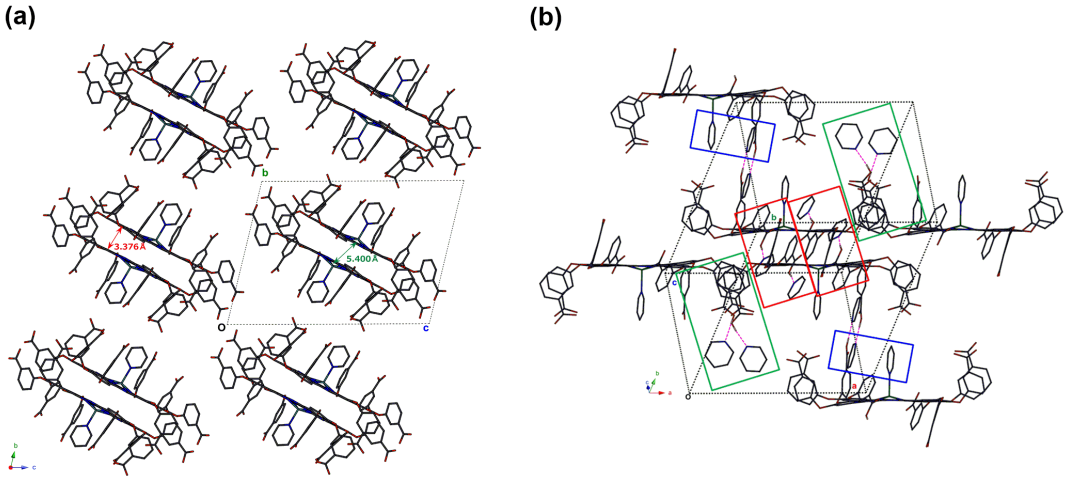

Figure 2. (a) Crystal packing diagrams of **2** viewed along the a axis. Hydrogen and solvents atoms are omitted for clarity(red: inter planar distance, green: Zn··Zn distance). (b) Various interactions in **2**. Red frame shows some π–π interactions between solvated pyridine molecules and those between phenoxy groups. Blue frame shows interactions between coordinated pyridine and the solvated pyridine molecule in the neighboring dimer. Green frame shows the interactions between solvated pyridine molecules and those between phenoxy groups that combine a dimer with the neighboring dimers.

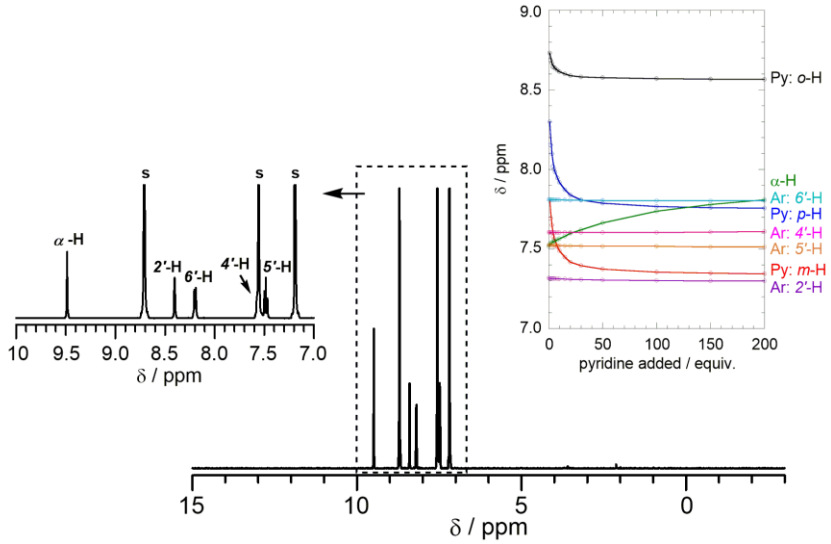

Figure 3. ^{1}H NMR spectrum of **1** in pyridine-d_5 at rt. Inset, change in chemical shifts of the proton signals as observed by the addition of pyridine into the acetone-d_6 solutions of **1** at rt.

We have then examined the solution properties of **1**. Although complex **1** is insoluble in nonpolar solvents such as $CHCl_3$, CH_2Cl_2 and C_6H_6, it shows a good solubility to polar organic solvents such as pyridine, acetone, and DMSO, allowing us to measure ^{1}H NMR, UV-Vis, and fluorescent spectra in these solutions. As shown in Figure 3, the ^{1}H NMR spectrum of **1** taken in pyridine-d_5 solution at room temperature exhibits well resolved signals. The HH COSY technique shown in Figure S3 unambiguously determines the signal assignments. The phenoxy proton signals appear at δ = 7.48 (*5'*-H), 7.56 (*4'*-H), 8.20 (*6'*-H), and 8.40 (*2'*-H) ppm and the α-proton signal of the phthalocyanine ring shows a sharp singlet at δ = 9.49 ppm. The carboxyl proton signal seems to be too broad to observe. Complex **1** is expected to have five-coordinate structure and should exhibit the signals for coordinated pyridine at rather upfield positions due to the ring current effect of the phthalocyanine ring. In order to directly observe these signals, the acetone-d_6 solution of **1** was titrated with pyridine. Figure 3 shows the titration curves obtained by plotting the ^{1}H NMR chemical shifts against equivalence of pyridine added. Pyridine signals were observed downfield, 8.73 (*o*-H), 8.30 (*p*-H), and 7.81 (*m*-H) ppm, when 1.0 equiv. of pyridine was added. These signals moved upfield and approached to the chemical shifts of free pyridine signals. The result strongly suggests that the added pyridine reacted with carboxylic acid moiety to form pyridinium ion. Coordination to the zinc(II) ion should follow after most of the carboxylic acid moieties are converted to carboxylate. The absence of the pyridine signals at the upfield positions should then be ascribed to the fast exchange between coordinated and free pyridine on the ^{1}H NMR timescale. In contrast to the pyridine signals, the *α*-H signal of phthalocyanine was observed upfield, 7.52 ppm, in acetone-d_6 solution and shifted downfield when pyridine was added. The result is a clear indication that the population of the aggregated species decreases on addition of pyridine.

The UV–Vis spectra of **1** were also taken in various solvents. In pyridine solution, the spectrum was typical for that of non-aggregated phthalocyanine; it exhibited a sharp Q band at 681 nm with $\varepsilon = 2.8\times10^5$ $M^{-1}cm^{-1}$ as shown in Figure 4. In contrast, the spectrum in acetone solution showed broad B and Q bands as given in Figure S4. Broad bands were sharpened, however, when pyridine was added. The result indicates that the aggregated species is converted to monomeric one by the addition of pyridine.

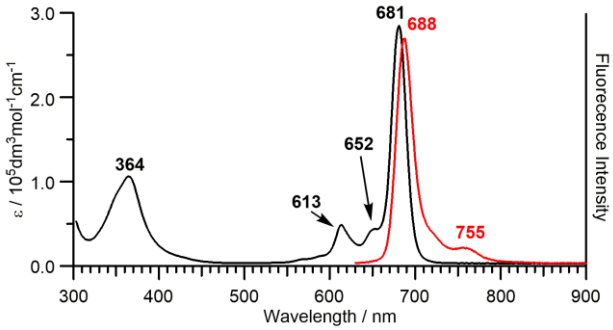

Figure 4. UV-Vis(black line) and fluorescence (red line) spectra of **1** in pyridine

The UV-Vis spectra of **1** were then examined in water. While the solid sample of **1** showed a low solubility to water, a clear solution was obtained by the addition of 1 % pyridine as shown in Figure S5(a). The spectrum thus obtained was essentially the same as that in pyridine solution, suggesting the formation of monomeric species. Although the solid sample of **1** was insoluble to water, it was soluble to the buffered aqueous solutions fixed at pH = 6.9 and 10.0. The increase in solubility of **1** in these buffered solutions is ascribed to the deprotonation of the eight carboxyl groups to form carboxylates. Although the solubility of **1** was greatly improved in the neutral and basic buffered solutions, the UV-Vis spectra given in Figure S5(b) and (c) exhibited broad B and Q bands. The results indicate that **1** exists as an aggregated form even in the buffered solutions. On the basis of these results, we have concluded that **1** exists as a monomeric form in aqueous solution when the following two conditions are satisfied; deprotonation of peripheral carboxyl groups and coordination of pyridine to the zinc ion.

Complex **1** displays a strong fluorescence bands at 688 and 755 nm (λ_{ex} = 613 nm) as shown in Figure 4. Thus, the Stokes shift is estimated to be 7 nm. The results suggest that the photo-inactive dimerized or polymerized species are not formed in pyridine solution due to the presence of eight carboxylate groups together with the axially coo orrdinated pyridine ligand.

In conclusion, we have synthesized four-coordinate [ZnPc(3-$CO_2H)_8$] (**1**) and pyridine ligated five-coordinate [ZnPc(3-$CO_2H)_8$(Py)]·8(Py) (**2**), and have succeeded in structural determination of the latter complex. Crystal structure of **2** is stabilized by O-H···N hydrogen bonds as well as π–π interactions between two pyridine molecules, and also between pyridine and phenoxy groups attached to phthalocyanine β-carbon atoms. Solution properties of **1** have been examined by means of ^{1}H NMR, UV–Vis, and fluorescent spectroscopy. On the basis of the spectroscopic studies, it was concluded the **1** exists as an aggregation form in neutral and basic aqueous solution, which is converted to the monomeric form by the addition of pyridine.

EXPERIMENTAL

Typical Procedure Scheme 1 shows the synthetic route to prepare **2**. We have slightly modified the reported methods.[5,6] Treatment of readily available 4,5-dichlorophthalonitrile (1.0 g, 5.3 mmol) with ethyl 3-hydroxybenzoate (1.40 g, 12 mmol) in the presence of K_2CO_3 (4.5 g, 33 mmol) gave 4,5-bis(3-ethoxycarbonylphenoxy)phthalonitrile in 97%. The phthalonitrile (0.45 g, 1.3 mmol) was cyclized using $Zn(OAc)_2 \cdot 2H_2O$ (0.14 g, 0.64 mmol) and DBU (0.2 mL) in 1-pentanol (10 mL) at 145 ºC for 24 h under N_2. Hydrolysis with NaOH in MeOH-H_2O (5:1) followed by the acidification with HCl aq. yielded the four-coordinate Zinc(II) complex (**1**), which was identified by ^{1}H NMR, UV-Vis, MALDI-TOF-Mass, and elemental analysis as described in the following section. Four-coordinate **1** was converted to pyridine ligated five-coordinate **2** by recrystallization from pyridine/hexane solution.

Analytical and spectroscopic data for 1

Anal. Calcd for $C_{88}H_{48}N_8O_{24}Zn$: C, 63.41; H, 2.90; N, 6.72%. Found: C, 62.95; H, 3.36; N, 6.40%. MALDI-TOF-Mass (positive): Calcd. for $[C_{88}H_{48}N_8O_{24}Zn]^+$: 1664.21. Found: 1664.19 *m/z*. ESI-TOF-Mass (MeOH, negative): Calcd. for $[C_{88}H_{48}N_8O_{24}Zn\text{-}2H]^{2-}$: 831.0964. Found: 831.0971 m/z. Calcd. for $[C_{88}H_{48}N_8O_{24}Zn\text{-}3H]^{3-}$: 553.7285. Found: 553.7319 *m/z*. Calcd. for $[C_{88}H_{48}N_8O_{24}Zn\text{-}4H]^{4-}$: 415.0435. Found: 415.0462 *m/z*. Calcd. for $[C_{88}H_{48}N_8O_{24}Zn\text{-}5H]^{5-}$: 331.8342. Found : 331.8361 *m/z*.

^{1}H NMR (pyridine-d_5, 500 MHz, r.t.): δ= 7.48 (*5'*-H, 8H, t), 7.56 (*4'*-H, 8H, m), 8.20 (*6'*-H, 8H, d), 8.40 (*2'*-H, 8H, s), and 9.49 (*α*-H, 8H, s) ppm. UV-vis (pyridine): λ_{max}(ε: x10^5 M^{-1}cm^{-1}) = 364 (1.0), 613 (0.5), 652 (0.4, sh), and 681(2.8) nm. Fluorescence (pyridine, λ_{ex} = 613 nm): λ_{max} = 688 and 755 nm.

Instrumentation and Materials UV-Vis absorption spectra were recorded in pyridine, acetone, and aqueous solution on a Shimadzu UV-3100 spectrometer. Measurement in aqueous solution was carried out in 25 mM phosphate buffer (pH 6.9) and 25 mM carbonate buffer (pH 10.0). Photoluminescence (PL) spectra were recorded in pyridine solution on a Shimadzu RF-5300PC spectrofluorometer with an excitation light of λ = 613 nm. ^{1}H NMR spectra ware recorded on a JEOL delta ECX-500 spectrometer operating at 500.1 MHz. Chemical shifts for ^{1}H NMR spectra were referenced to pyridine-d_5 (δ = 7.19 ppm) and acetone-d_6 (δ = 2.04 ppm). MALDI-TOF-MS spectra were recorded on a Bruker Daltonics pAutoflex-T1 and bioMérieux VITEK® MS. ESI-TOF-MS spectra were recorded on a Bruker microTOF using negative mode for acetonitrile solutions by using sodium formate as reference. Unless otherwise noted, materials obtained from commercial suppliers were used without further purification. Crystals suitable for X-ray structure analysis were obtained from pyridine/*n*-hexane mixed-solvent solutions for **2**. X-Ray measurement of the single crystals were done with Rigaku VariMax Saturn-724 (1.2 kW Mo rotating anode) at 100 K for **2**. Single crystals for X-ray analysis were obtained by the diffusion method. X-Ray diffraction data were processed using Crystal Clear 1.6.3 followed by CrystalStructure Ver. 4.0.1. The structures were solved using SUPERFLIP and expanded using the

Fourier technique.[9] All calculations were performed using the CrystalStructure crystallographic software package.[10] The structure was refined on F^2 by full-matrix least-squares using the SHELXL-2014 program package.[11] Crystal data and details concerning the data collection are given in Table S1. All non-hydrogen atoms were refined anisotropically. Hydrogen atoms were located in the calculated positions and refined by using riding models. Large electron peaks near the special position (0 0 0) were found probably due to the disordered solvent molecule. We failed to model them properly. Therefore, the original diffraction data were modified by the PLATON SQUEEZE technique in order to refine the structure without the disordered solvent molecules.[12] Final structures were validated by Platon CIF check. Selected bond distances and angles are list in Table 1. Crystallographic data for complex **2** reported in this paper have been deposited with the Cambridge Crystallographic Data Centre, CCDC no. 1509837. Copies of the information may be obtained free of charge from: The Director, CCDC, 12 Union Road, Cambridge, CB2 1EZ, UK (fax: +44-1223-336033; e-mail: deposit@ccdc.cam.ac.uk or via http://www.ccdc.cam.ac.uk/data _request/cif).

ACKNOWLEDGEMENTS

This work supported by JSPS KAKENHI Grant Number 15K17825(S.M) and the Uehara Memorial Foundation 2015(A.N). The authors are grateful to Ms. Michiko Egawa (Shimane University) for her measurements of elemental analysis. The X-ray diffraction experiment was performed at Advanced Research Support Center, Ehime University. Thanks are due to the Research Center for Molecular-Scale Nanoscience, the Institute for Molecular Science (IMS), Okazaki, Japan.

REFERENCES

1. F. H. Moser and A. L. Thomas, The Phthalocyanines, Vol. I, CRC Press, Boca Raton, FL, 1983.
2. The Porphyrin Handbook, Vol. 19, ed. by K. M. Kadish and K. M. Smith, R. Guilard, Academic Press, San Diego, 2003.
3. K.-Y. Law, *Chem. Rev.*, 1993, **93**, 449.
4. The Phthalocyanines, Properties and Applications, Vol. 4, ed. by C. C. Leznoff and A. B. P. Lever, VCH, New York, 1996.
5. W. Liu, T. J. Jensen, F. R. Fronczek, R. P. Hammer, K. M. Smith, and M. G. H. Vicente, *J. Med. Chem.*, 2005, **48**, 1033.
6. C.-F. Choi, P.-T. Tsang, J.-D, Huang, E. Y. M. Chan, W.-H. Ko, W.-P. Fong, and D. K. P. Ng, *Chem. Commun.*, 2004, 2236.
7. F.-J. Yang, X. Fang, H.-Y. Yu, and J.-D. Wang, *Acta Cryst.*, 2008, **C64**, m375.
8. T. Fukuda, S. Homma, and N. Kobayashi, *Chem. Eur. J.*, 2005, **11**, 5205.

9. L. Palatinus and G. Chapuis, *J. Appl. Cryst.*, 2007, **40**, 786.
10. CrystalStructure Ver. 4.1: Crystal structure analysis package, Rigaku, Tokyo, Japan and Rigaku/MSC (The Woodlands, TX, USA), 2014.
11. G. M. Sheldrick, *Acta Cryst.*, 2015, **A71**, 3.
12. A. L. Spek, *Acta Cryst.*, 2015, **C71**, 9.